International Journal of Control

ISSN: 0020-7179 (Print) 1366-5820 (Online) Journal homepage: https://www.tandfonline.com/loi/tcon20

Interactive computer-aided control design using quantitative feedback theory: the problem of vertical movement stabilization on a high-speed ferry

J. M. Díaz , S. Dormido & J. Aranda

To cite this article: J. M. Díaz , S. Dormido & J. Aranda (2005) Interactive computer-aided control design using quantitative feedback theory: the problem of vertical movement stabilization on a high-speed ferry, International Journal of Control, 78:11, 813-825, DOI: 10.1080/00313020500171657

To link to this article: https://doi.org/10.1080/00313020500171657

Published online: 20 Feb 2007.

Submit your article to this journal

Article views: 80

View related articles

Citing articles: 1 View citing articles

Full Terms & Conditions of access and use can be found at
https://www.tandfonline.com/action/journalInformation?journalCode=tcon20

International Journal of Control
Vol. 78, No. 11, 20 July 2005, 813–825

Taylor & Francis
Taylor & Francis Group

Interactive computer-aided control design using quantitative feedback theory: the problem of vertical movement stabilization on a high-speed ferry

J. M. DÍAZ, S. DORMIDO* and J. ARANDA

Department de Informática y Automática, ETSI Informática, UNED, 28040 Madrid, Spain

(*Received 9 December 2004; in final form 19 May 2005*)

In a first approximation, the vertical acceleration associated with pitch motion can be considered as the main cause of motion sickness, which is without a doubt one of the most unpleasant disadvantages of maritime transport. The reduction of motion sickness can be stated as a monovariable regulation problem of a highly perturbed system. This work presents the design of a monovariable robust controller with quantitative feedback theory (QFT) for reducing the vertical movement on a high-speed ferry. The different stages of QFT methodology have been done with the help of the software tool QFTIT (Quantitative Feedback Theory Interactive Tool). This is a free software tool that is characterized by its ease of use and interactive nature. The designed regulator is validated experimentally in sea behaviour trials with a scaled down replica 1/25 the size of a high-speed ferry. The designed regulator is also compared with a gain-scheduling scheme using a proportional and derivative controller (PD).

1. Introduction

Fast Ferries are widely used on regular maritime lines for transporting passengers and cars. Just in Europe in 2000, 82.6 million passengers and 12.8 million cars were transported by these kinds of vehicles. Moreover, the construction and exploitation of fast ferries is a growing market, with over 200 companies currently operating 1,250 fast ferries.

Passenger comfort is one of the most important factors that maritime transport firms must improve in order to increase their competitiveness with air transport. Motion sickness is without a doubt one of the most unpleasant disadvantages of maritime transport. Obviously, a decrease as far as possible in this motion sickness will lead to greater comfort and safety.

Vertical accelerations are the main cause of motion sickness. These vertical accelerations are associated with heave and pitch motions that are produced as the waves fall against the ship. Therefore, a ferry subjected to waves behaves like a highly perturbed system. The regulation problem consists of designing a robust regulator to control the motion of the right mechanical actuators (flaps, T-foil) and attenuate, as far as possible, the ferry's vertical dynamic motions (heave and pitch) to reduce motion sickness incidence (MSI), the measurement used for quantifying motion sickness suffered by passengers.

In a first approximation, the vertical acceleration associated with pitch motion can be seen to be the sole cause of motion sickness. The multivariable robust regulation problem can therefore be reduced to a monovariable one where the pitch motion is damped by the right control of the T-Foil. Thus, it is possible to use the flaps to correct the course deviations, or even not to install them.

The main specification of this regulation problem ''Reducing MSI as far as possible'' is very generic. Therefore, it is possible at first sight to use different robust control techniques to solve this problem. For instance, a suitable technique for designing a robust regulator is quantitative feedback theory (QFT). The design procedure using QFT has been described in a

*Corresponding author. Email: sdormido@dia.uned.es

International Journal of Control
ISSN 0020–7179 print/ISSN 1366–5820 online © 2005 Taylor & Francis Group Ltd
http://www.tandf.co.uk/journals
DOI: 10.1080/00313020500171657

wide variety of articles and books (Horowitz 1963, 1992, 2001, Houpis *et al*. 1992, Houpis and Rasmussen 1999, Yaniv 1999). QFT is an engineering control design methodology that uses frequency-domain concepts to satisfy performance specifications and handle plant uncertainty. QFT is based on the observation that feedback is needed mainly when the plant is uncertain and/or when there are disturbances acting on the input and/or the output of the plant. The benefits of QFT are summarized in § 4.1.

There are currently many different tools all aimed at helping the designer implement the different stages of QFT methodology. The most widespread and well known of all the existing CAD tools is the QFT frequency domain control design toolbox (FDCDT) written in Matlab (Borghesani *et al*. 1995).

Recently, the Quantitative Feedback Theory Interactive Tool (QFTIT) for single-input–single-output (SISO) has been developed in Sysquake (Pyguet 1999) in an attempt to help users learn and understand the basic concepts involved in QFT design.

The main advantages of QFTIT compared to FDCDT are its ease of use and interactive nature. All that the end-user has to do is to place the mouse pointer over the different items that the tool displays on the screen. Any actions carried out on the screen are immediately reflected on all the graphs generated and displayed by the tool. This allows users to visually perceive the effects of their actions during the controller design. The reader is cordially invited to visit the website http://ctb.dia.uned.es/asig/qftit/ to experience the interactive features of QFTIT.

The philosophy of interactive design with instantaneous performance display offers two main advantages (Dormido 2003, 2004) when compared with the traditional procedure (non-interactive approach). First, right from the beginning it introduces the control engineer to a tight feedback iterative design loop. Designers can identify the bottlenecks of their designs very easily and attempt to fix them. Second, and this is probably even more important, not only is the effect of the manipulation of a design parameter displayed, but its direction and amplitude also become apparent. The control engineer learns quickly which parameter to use and how to push the design in the direction of fulfilling better tradeoffs in the specifications. Fundamental limitations of the system and the type of controller are therefore revealed (Åström 1994, 2000) which make it possible to find an acceptable compromise for all the performance criteria. Using this interactive approach we can learn to recognise when a process is easy or difficult to control.

QFTIT is an interactive tool to learn QFT but it can also be used to solve real problems of controller design. Thus, this work presents the design of a monovariable robust regulator with QFTIT for the reduction of motion sickness incidence on a high-speed ferry. The designed regulator is validated experimentally using sea behaviour trials with a physical scale model 1/25 size of a high-speed ferry. It is also compared with a previous non-robust design: a gain-scheduling scheme with a PD controller (Díaz 2002).

This monovariable design will obviously reduce MSI less than a multivariable design (Aranda *et al*. 2005). However, the realization of the QFT monovariable design was demanded for the naval industry, which prefers to install few mechanical actuators in the hull.

On the other hand, the realization of a QFT monovariable design is very advisable as a previous step to the successful realization of a QFT multivariable design. It gives valuable information and experience about how to translate the specifications to the frequency domain, and how to try to do the loop-shaping in the Nichols diagram.

The structure of this paper is as follows: first, the process model is described in § 2. Then, the control problem is stated in § 3. Next, the design of a robust regulator using QFTIT for the reduction of vertical movement on a high-speed ferry is described in § 4. After, the experimental validation of this design is commented on in § 5. Finally, the conclusions are set out in § 6.

2. Process model

In Aranda *et al*. (2004), continuous linear models of the vertical dynamics of a high-speed ferry were identified for different navigation speeds (20, 30 and 40 knots). These models can be considered as acceptable since they adjust well to the amplitude and phase of the experimental data. Their time simulations with regular and irregular waves present only a small average quadratic error when compared with the experimental time series.

Moreover, two kinds of mechanical actuators were designed (see figure 1): a pair of fins on the bow (T-Foil) and two flaps on the stern. Both linear and non-linear models were obtained in Cruz *et al*. (2004) for these actuators.

The process model is taken to be the linear model of the vertical dynamics of a high-speed ferry together with the non-linear model of the actuators. This is a multivariable model with two manipulated variables, the set-point of the flaps position u_F and the set-point of the T-Foil position u_T. The process has two controlled variables, the heave motion h and the pitch motion p. There is also one disturbance, the wave height w.

If the saturation of the actuators is not very high, a linear model of the actuators for control of position can be considered (Esteban *et al*. 2000). In this instance

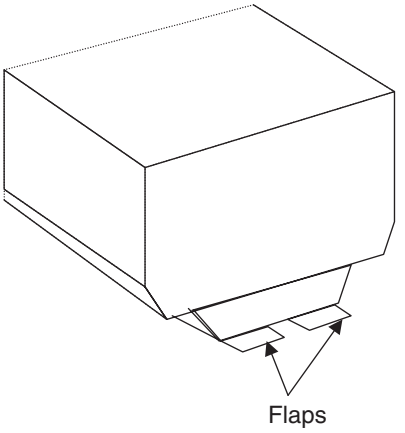

(a)

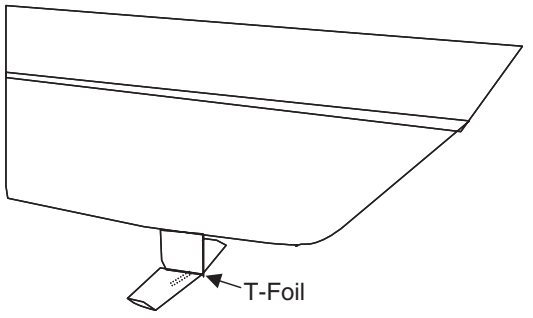

(b)

Figure 1. Mechanical actuators of the scaled down replica 1/25 the size of a fast ferry: (a) Two flaps on the stern; (b) T-Foil on the bow.

it is possible to represent the process using the following pair of equations

$$h(s) = P_{FH}(s) \cdot u_F(s) + P_{TH}(s) \cdot u_T(s) + P_{WH}(s) \cdot w(s) \quad (1)$$

$$p(s) = P_{FP}(s) \cdot u_F(s) + P_{TP}(s) \cdot u_T(s) + P_{WP}(s) \cdot w(s), \quad (2)$$

where the $P_{ij}(s)$ are transfer functions.

On the other hand, the vertical acceleration associated with the heave motion a_{VH} is given by the following expression

$$a_{VH} = \cos p \cdot \frac{d^2h}{dt^2}. \quad (3)$$

While the vertical acceleration associated with the pitch motion a_{VP} is given by

$$a_{VP} = -x \cdot \frac{d^2p}{dt^2}, \quad (4)$$

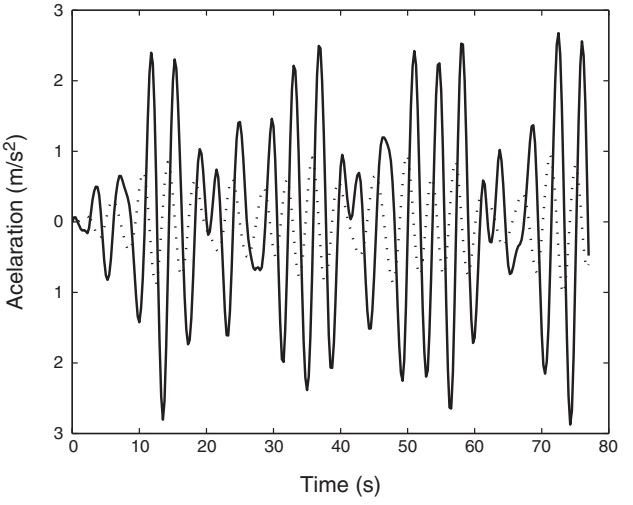

Figure 2. Time series of a_{VP} (solid line) and a_{VH} (broken line) measured in El Pardo Model Basin (Spain) with a physical scale model 1 : 25 size of a fast ferry. Navigation conditions (real scale): ship speed U = 40 knots; sea state number SSN = 4 and $x = 40$ m.

where x is the distance from the point of the ship where the accelerometer is placed at the centre of gravity. Therefore, the total vertical acceleration a_V is given by the sum of the two components a_{VP} and a_{VH}

$$a_V = a_{VP} + a_{VH}. \quad (5)$$

The magnitude of the acceleration a_{VP} is usually several times greater than the acceleration a_{VH} (see figure 2). Thus in a first approximation it is possible to consider that the vertical acceleration is only associated with the pitch motion.

The pitch motion defined by equation (2) can be written as

$$p(s) = p_F(s) + p_T(s) + p_W(s), \quad (6)$$

where

$$p_F(s) = P_{FP}(s) \cdot u_F(s)$$
$$p_T(s) = P_{TP}(s) \cdot u_T(s)$$
$$p_W(s) = P_{WP}(s) \cdot w(s).$$

It can be observed that the pitch motion $p(s)$ is decomposed into three associated components: (a) the Flap motion $p_F(s)$; (b) the T-Foil motion $p_T(s)$; (c) the waves $p_W(s)$. Of these three components, the main contribution to the pitch motion is the component associated with the waves $p_W(s)$. Furthermore, the

component $p_T(s)$ is much greater than the component $p_H(s)$ when the flaps are maintained in a fixed angular position (Díaz 2002). In this case, it might be possible not to consider the component $p_H(s)$. Equation (6) can thus be expressed as follows:

$$y(s) = P(s) \cdot u(s) + d(s), \tag{7}$$

where $y(s) = p(s)$, $P(s) = P_{TF}(s)$, $u(s) = u_T(s)$ and $d(s) = P_{WP}(s) \cdot w(s)$.

The perturbation term $d(s)$ belongs to the set of permissible perturbations $\mathcal{D}$ on a fast ferry. This set $\mathcal{D}$ is usually defined by the waves whose sea state number (SSN) is less or equal to 5, i.e. the significant height of the waves is less or equal to 3.25 meters.

In order to study robustness properties, a family of plants $\mathcal{P}$ defined as a transfer function with parametric uncertainties in its coefficients was obtained in Díaz (2002) from the linear model of the process at different ship speeds (20, 30 and 40 knots). Its expression is

$$\mathcal{P} = \left\{ \begin{array}{ll} P(s) = \dfrac{K(s+a)\cdot(s+b)}{(s+103.2)\cdot(s+1.8)\cdot(s+c)\cdot(s^2+ds+e)} & \\ K = [-0.87,\ -0.65] & a = [-7.85,\ -6.67] \\ b = [0.026, 0.042] & c = [0.44, 0.49] \\ d = [0.86, 0.97] & e = [2.59, 2.80] \end{array} \right\}. \tag{8}$$

The nominal plant $P_0 \in \mathcal{P}$ is chosen at a ship speed of 40 knots, a case of special interest for navigation. Its expression is

$$P_0(s) = \frac{-0.87(s-7.85)\cdot(s+0.042)}{(s+103.2)\cdot(s+1.8)\cdot(s+0.49)\cdot(s^2+0.86s+2.8)}. \tag{9}$$

3. Statement of the regulation problem

The motion sickness that people suffer when they travel by ship is due to the vertical accelerations associated with the heave and pitch motions induced by the waves. The quantification of motion sickness is a complicated problem, since the vertical accelerations that cause it affect every individual differently. It is necessary to resort to statistical methods on a large number of analysed subjects. A classic experiment on sea motion sickness is presented in O'Hanlon and McCauley (1974), who defined motion sickness incidence (MSI) as the percentage of subjects that were sick within two hours of navigation and they expressed it mathematically as

$$\mathrm{MSI} = 100\left[0.5 + erf\left(\frac{\log_{10}(\mathrm{WVA}/g) - \mu_{\mathrm{MSI}}}{0.4}\right)\right]. \tag{10}$$

WVA is the average value of the total vertical acceleration a_V at 40 meters ahead of the mass center for a total of N points

$$\mathrm{WVA} = \frac{1}{N}\sum_{i=1}^{N} |a_v(t_i)|. \tag{11}$$

Moreover, μ_{MSI} in equation (10) is defined by the equation

$$\mu_{\mathrm{MSI}} = -0.819 + 2.32 \cdot (\log_{10}\ \omega_e)^2, \tag{12}$$

where ω_e is the encounter frequency, which is the relative frequency with which the waves fall against a ship.

From the study of the dominant wave encounter frequency component in each sea state, and from the study of the wave spectrum, it can be deduced that the right range of frequencies to minimize MSI as far as possible is $\Omega = [1, 2.5]$ rad/sec.

In accordance with equation (10), minimizing MSI implies reducing WVA. Therefore, reducing WVA implies damping the pitch and heave motion. In § 2, it was shown that total vertical acceleration causing motion sickness can be considered in a first approximation as solely associated with the pitch motion. Accordingly, the design of a monovariable regulator $C(s)$ to reduce MSI is justified. The system considered is shown in figure 3.

A decrease in pitch motion is equivalent to reducing the system's sensitivity to the waves. From the point of view of frequency domain this means working with the sensitivity function S of the output (pitch) y to the perturbation (waves) d

$$S(s) = \frac{y(s)}{d(s)} = \frac{1}{1 + P(s)(s)}. \tag{13}$$

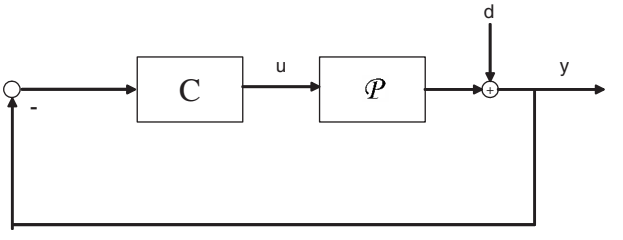

Figure 3. SISO regulation structure used to reduce MSI.

Then, the problem to solve may be formally stated as follows.

Problem 1: Consider the system shown in figure 3. Design a controller C, so that for all $P \in \mathcal{P}$ the system is stable and for all disturbance $d \in \mathcal{D}$ and frequency $\omega \in \Omega$ the magnitude of the sensitivity function S is bounded by the specification W_d

$$\left|S(j\omega)\right| \leq W_d(\omega). \tag{14}$$

The more negative the magnitude in decibels of S in the range of frequencies Ω considered, the greater the perturbation rejection that will be obtained, and therefore the greater the reduction in MSI. The key for establishing this perturbation rejection specification is to appropriately fix $W_d(\omega)$, analytically or numerically, i.e. impose some higher bounds for $|S|$ that guarantee the following conditions for every plant $P \in \mathcal{P}$ and for every perturbation $d \in \mathcal{D}$.

(1) Maximum reduction possible in MSI within the range of frequencies Ω.
(2) Robust stability of the system.

There is no analytical expression that relates MSI to $|S|$. It is therefore neither direct nor trivial to ascertain what MSI reduction percentage will be achieved for some function S. The method thus has to be indirect using approximation. It is obvious that given a controller C, with each one of the plants $P \in \mathcal{P}$, a reduction percentage in MSI will be obtained. If the controller is robust it must ensure a minimum percentage irrespective of the $P \in \mathcal{P}$ considered.

Nevertheless, $W_d(\omega)$ cannot be chosen so that $|S|$ is arbitrarily small, because the system presents two important limitations: the family of plants $\mathcal{P}$ is a non-minimum phase (NMP), and the saturation of the actuators.

The family of plants $\mathcal{P}$ (see equation (8)) has one zero on the right half of the complex plane. The benefits of feedback for NMP plants are limited, in the sense that no closed loop specifications can be achieved using a linear time invariant controller. The open loop crossover frequency of an NMP system has an upper bound (Horowitz 1992, Yaniv 1999), hence the amplitude of the open loop frequencies below the cross-over frequency is also bounded. This limitation is clearly shown in the loop-shaping stage of the QFT methodology in the resolution of the Problem 1. If $W_d(\omega)$ is chosen so that $|S|$ is too small, the disturbance rejection bounds in the Nichols chart will be far away from the 0 dB axis and it will not be possible to find a controller that can fulfil this specification without making the system unstable.

The saturation of the actuator is a factor that must be taken into account when $W_d(\omega)$ is chosen. This is because the larger the perturbation rejection, the greater the saturation that will be obtained, negating the benefits of the feedback.

A good starting point for the selection of $W_d(\omega)$ is to consider the sensitivity functions S that are obtained when the process is controlled with a gain-scheduling scheme using a PD controller (Díaz 2002) at ship speeds of U = 20, 30, 40 knots. With this gain-scheduling scheme, some acceptable reductions in MSI were obtained. For example, at nominal conditions the PD controller was

$$C = \frac{10.5\,s^2 + 7.4}{0.13\,s + 1}. \tag{15}$$

Furthermore, a MSI reduction percentage of about 31.8% was obtained in simulation.

Thus, bearing in mind the conditions to fulfil and the limitations to consider, an iterative trial-and-error method was used to select $W_d(\omega)$. The $W_d(\omega)$ selected are shown in table 1.

According to Yaniv (1999), one way of assuring the robust stability of the system is to fulfil the following specification in the resolution of Problem 1

$$\left|\frac{C(j\omega)\cdot P(j\omega)}{1 + C(j\omega)\cdot P(j\omega)}\right| \leq W_s \quad \forall\, P \in \mathcal{P} \quad \forall\, \omega. \tag{16}$$

W_s is a constant value that must be larger than 1.

Specification (16) draws closed bounds in the Nichols chart around the critical point $(-180^\circ, 0\,\text{dB})$. These bounds are very useful in the loop-shaping stage as a visual reference so that the open loop does not enter into the forbidden zone of the Nichols chart (phases less than -180° and magnitude larger than 0 dB) and secure some stability margin. Several previous trial-and-error iterations showed that a good selection is $W_s = 1.2$.

In Chait and Yaniv (1993) it is shown that the value W_s is related to the gain margin GM and to the phase

Table 1. Specification $W_d(\omega)$.

ω [rad/sec]	$W_d(\omega)$ [dB]
1.00	−0.14
1.25	−0.21
1.50	−0.60
2.00	−0.75
2.50	−0.28

margin PM by the following expressions

$$GM = 1 + \frac{1}{W_s} \tag{17}$$

$$PM = 180^\circ - \frac{180^\circ}{\pi} \mathrm{a}\cos\left(\frac{0.5}{W_s^2} - 1\right). \tag{18}$$

Then, with $W_s = 1.2$ specification (16) assures a phase margin $PM \geq 50^\circ$ and a gain margin $GM \geq 1.8$.

4. Design of the controller using QFTIT

QFTIT (http://ctb.dia.uned.es/asig/qftit/) was the software tool chosen to help us implement the different QFT stages in order to design a robust monovariable controller C that solves Problem 1. This tool divided the implementation of a QFT design into four stages: Template computation, Specifications, Loop-shaping and Validation. In this section, first of all, the basic concepts of QFT are briefly explained. Then, the realization of each of the QFT stages using QFTIT for solving Problem 1 is described.

4.1. *Basic concepts of quantitative feedback theory*

QFT was created and developed by Horowitz (1963). This is a methodology used for designing control systems that include plant uncertainties. The plant input and/or output are subject to external disturbances and are affected by measurement noise. The benefits of QFT may be summarised as follows:

- The outcome is a robust controller design that is insensitive to plant variation.
- There is only one design for the full envelope and it is not necessary to verify plants inside templates.
- Any design limitations are clear at the very beginning.
- There is less development time in comparison to other robust design techniques.
- QFT generalises classical frequency-domain, loop-shaping concepts to cope with simultaneous specifications and plants with uncertainties.
- The amount of feedback is adapted to the amount of plant and disturbance uncertainty and the performance specifications.
- The design trade-offs in every frequency are transparent between stability and performance specifications. It is possible to determine what specifications are achievable during the early stages in the design process.
- The redesign of the controller for changes in the specifications can be done very fast.

The blocks diagram shown in figure 3 illustrates the basic idea behind QFT applied to a SISO regulation system. $\mathcal{P}$ is a family of plant transfer functions. The output y of $\mathcal{P}$ is subjected to a disturbance $d \in D$. C is the regulator which, depending on the distance of y from the zero value, generates a control signal u over $\mathcal{P}$. The QFT method takes into consideration the quantitative information of the plant's uncertainty, robust operation requirements, expected disturbance amplitude and the associated damping requirement.

The controller C must be designed in such a way that the set of possible outputs y, which are a consequence of plant uncertainties $\mathcal{P}$, are near to zero. Thus, the effects of the disturbance d are very small. The design is done using a Nichols diagram where a discreet set of trial frequencies Ω_1 is defined. This set is taken around the desired crossover frequency. As we are treating a family of plants instead of a single plant, the magnitude and phase of the plants in each frequency correspond to a set of points in the Nichols diagram. These sets of points form a connected region or a set of disconnected regions called "template". $\mathcal{T}(\omega_i)$ denotes a template computed at the frequency $\omega_i \in \Omega_1$. A large template implies a greater uncertainty for a given frequency. The templates and the working specifications are used to define the domain bounds within the frequency domain. The domain bounds set the limit of the frequency response of the open loop system.

Each specification contains bound definitions. Bounds are calculated using the corresponding templates and specifications. All the bounds computed at the same frequency $\omega_i \in \Omega_1$ associated at the different specifications are intersecting to generate a final bound $\mathcal{B}(\omega_i)$ which includes the most restrictive regions of all the considered bounds.

The controller is designed by means of a loop-shaping process in the Nichols diagram. This diagram sketches the intersection of the bounds calculated for each of the trial frequencies and the characteristics of the open loop nominal transfer function $L_0(j\omega) = C(j\omega) \cdot P_0(j\omega)$.

The design is carried out by adding gains, poles and zeroes to the nominal plant frequency response in order to change the shape of the open loop transfer function. By doing so, the boundaries $\mathcal{B}(\omega_i)$ $\omega_i \in \Omega_1$ are maintained for each of the trial frequencies Ω_1. The controller is the set of all the aforementioned items (gain, poles and zeroes).

The last step for the QFT design is analysis and validation which includes not only analysis in the frequency domain but also simulations in the time domain of the resulting closed loop system.

4.2. *Stage 1: Template computation*

During this stage, the user defines the plant $\mathcal{P}$ by configuring the uncertainty of its components. Furthermore, the user also selects the set of trial frequencies Ω_1. The templates $\mathcal{T}(\omega_i)$ $\omega_i \in \Omega_1$ are simultaneously computed and shown while the user does these actions. QFTIT implements the algorithm by Gutman *et al.* (1995) for the calculation of templates.

According to the disturbance rejection specification (see table 1) and the robust stability specification (16), a possible set of trial frequencies is

$$\Omega_1 = \{1, 1.25, 1.5, 2, 2.5, 10\}\,(\text{rad/s}). \tag{19}$$

The frequencies Ω_1 can be introduced in QFTIT using its area template frequency vector (see figure 4). There is a horizontal axis ω representing radian per seconds. It is possible to add, remove and change the frequencies of Ω_1. Each of these frequencies is represented by a vertical segment with an associated colour code that can be moved along the ω axis.

In Problem 1, the elements of the plant (8) are a gain, two simple zeroes, three simple poles and a pair of complex poles. One possible way of introducing them into QFTIT is using their areas (see figure 4) operations over plant P and uncertainty plant description.

The area operations over plant P (see figure 4) is used to select the type of plant element (real-pole, real-zero, complex-pole, complex-zero, integrator) on which we want to perform some type of action (move, add or remove) in the uncertainty plant description area. It is also possible to configure each element by using two sliders: the uncertainty of the delay and the gain of the plant, i.e. the specification of the minimum, maximum and nominal values. For the plant (8) the slider associated with the gain would have to be moved in order to configure its minimum value $k_{\min} = -0.87$, its maximum value $k_{\max} = -0.65$ and its nominal value $k_{\text{nom}} = -0.87$.

The uncertainty plant description area (see figure 4) is used to graphically design the configuration of the uncertainty of the plant poles and zeroes. This operation is carried out with the use of the mouse over the selected pole or zero element. For simple zeroes or poles the uncertainty is represented by a segment, whilst for complex zeroes and poles it is represented by a circular sector limited by the maximum and minimum values of the damping factor and the natural frequency of each complex item (pole or zero). Both representations include the extreme values as well as the nominal value.

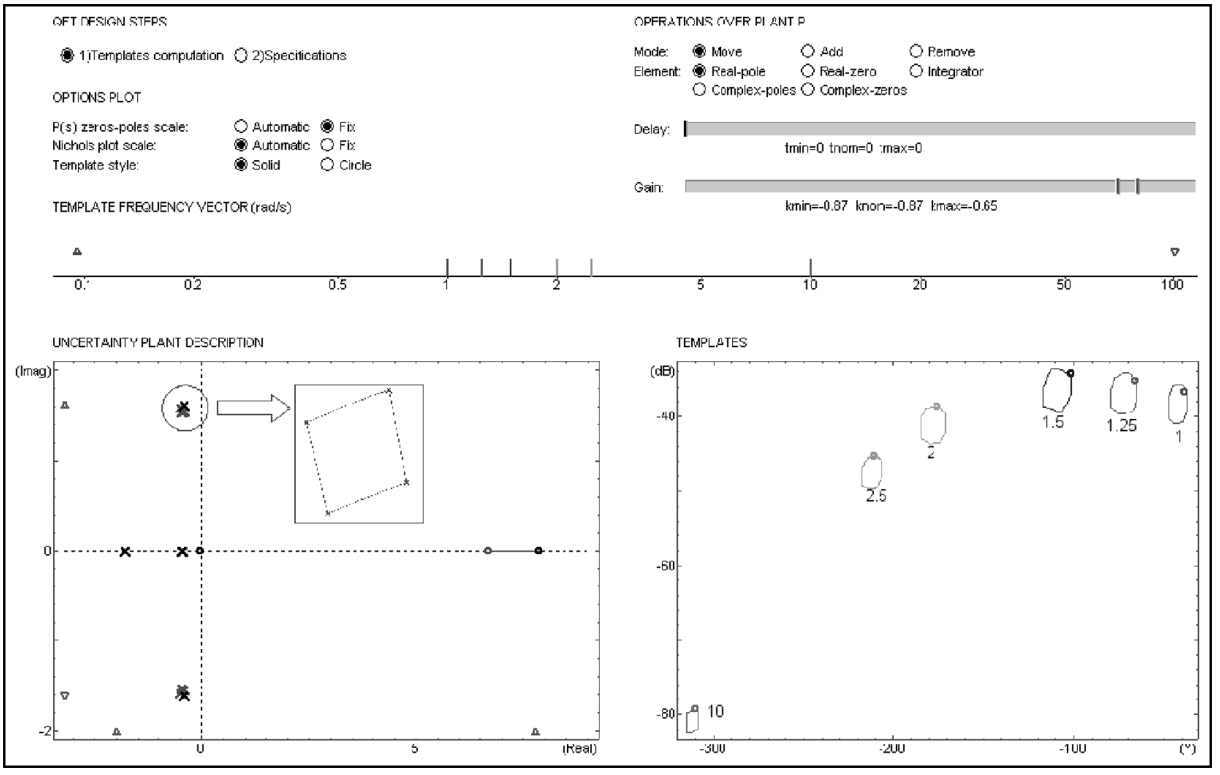

Figure 4. Aspect of the QFTIT window after stage 1 (Template Computation) for Problem 1. In the uncertainty plant description area has been included a zoom in the uncertainty region of the complex pole of the plant.

For Problem 1, according to the plant defined in (8), by selecting the adequate options in the operations over plant P area, it would be possible to add two simple zeroes ($s=-a, s=-b$), three simple poles ($s=-103.2, s=-1.8, s=-c$) and a pair of complex poles ($s=-d \pm j\cdot\sqrt{d^2-4\cdot e}$) in the uncertainty plant description area and to configure the uncertainty (a, b, c, d, e) of these elements and their nominal values (see equation (9)) by dragging the mouse.

The area templates show a Nichols diagram that includes the templates calculated for the set of frequencies defined in Ω_1. Problem 1 (see figure 4) shows six templates, each with the colour associated with the corresponding frequency in the set Ω_1.

4.3. *Stage 2: Specifications*

During this stage, the user selects and configures the specifications that their design must fulfil. QFTIT has implemented six different types of specifications (see table 2). Each selected specification must configure the value of its associated W_{si} $i=1,\ldots,6$ and select the frequencies under which each specification must be verified. There is also a simultaneous generation of associated bounds for each specification.

In Problem 1 there are two specifications: robust stability specification (Type 1) and disturbance rejection at plant output (Type 2). If Type 1 specification is selected and activated in the specification type zone (see figure 5), then it is possible to configure the value of the constant W_s by simply dragging the slider from value 1 to the desired value 1.2. Just under the slider there is a display showing the value of the gain margin ($GM \geq 1.8$) and the phase margin ($PM \geq 49.2^\circ$) obtained. It is also possible to view simultaneously and interactively how the specification modulus is being modified in the Bode diagram and how the associated bounds change in the Nichols diagram.

Table 2. Specifications implemented in QFTIT.

Type	Specification
1. Robust stability	$\left\lvert\frac{P\cdot C}{1+P\cdot C}\right\rvert \leq W_{s1}$
2. Disturbance rejection at plant output	$\left\lvert\frac{1}{1+P\cdot C}\right\rvert \leq W_{s2}$
3. Disturbance rejection at plant input	$\left\lvert\frac{P}{1+P\cdot C}\right\rvert \leq W_{s3}$
4. Control effort	$\left\lvert\frac{C}{1+P\cdot C}\right\rvert \leq W_{s4}$
5. Tracking bandwidth	$\left\lvert\frac{P\cdot C}{1+P\cdot C}\right\rvert \leq W_{s5}$
6. 2-DOF tracking	$W_{s6a} \leq \left(\left\lvert\frac{P\cdot C}{1+P\cdot C}\right\rvert\right) \leq W_{s6b}$

The specification of disturbance rejection at plant output (Type 2) for Problem 1 (see table 1) is given as a vector whose components are the values that the specification must take in dB at different frequencies. These kinds of specifications are called point-to-point (PP) in QFTIT. Thus, the configuration of this specification given in table 1 is as follows: first, it is necessary to select and activate the Type 2 specification in the specification type zone. Second, it is necessary to select the PP mode in the $W(s)$ frequency-domain specification zone. The $W(s)$ magnitude specification zone displays circles in different colours placed in the trial frequencies of the specification and with a value of 0 dB. Users can configure by dragging the mouse pointer over the modulus points to the chosen value. This will simultaneously update the bounds associated with this specification in the Nichols diagram (see figure 6).

In QFTIT the final bounds $\mathcal{B}(\omega_i)$ $\omega_i \in \Omega_1$ associated at the intersection of the two configured specifications are immediately displayed in the Nichols plot zone by selecting the option intersection in the option plot zone.

4.4. *Stage 3: Loop shaping*

During this stage, the user performs the synthesis of the controller $C(s)$ in the Nichols diagram by shaping the open loop transfer function L_0 in order to maintain the boundaries $\mathcal{B}(\omega_i)$ $\omega_i \in \Omega_1$. The main manipulation that the user can perform within this area of the programme is the displacement of L_0 in certain directions depending on the selected controller item in the operations over controller C zone.

The changes made to L_0 in the Nichols diagram are immediately reflected in an interactive way on the zeroes-poles map corresponding to $C(s)$ as well as in the symbolic expression of the transfer function. Likewise, the interactions performed by the user on the zeroes-poles map of the controller will be reflected in the Nichols diagram. Thus, the user has a very interactive and flexible tool to perform the synthesis of the controller.

Figure 7 displays the aspect of the QFTIT window after the loop-shaping stage. The Nichols diagram shows the intersection of the bounds associated with the established specifications and the final L_0. It can be observed how the points $L_0(j\omega_i)$ fulfil the boundaries $\mathcal{B}(\omega_i)\omega_i \in \Omega_1$.

The expression of the designed controller is

$$C(s) = 1.1\cdot 10^5 \cdot \frac{(s+0.5)\cdot(s+0.8)}{(s+32)\cdot(s^2+2\cdot 0.2\cdot 26.5\cdot s+26.5^2)}. \tag{20}$$

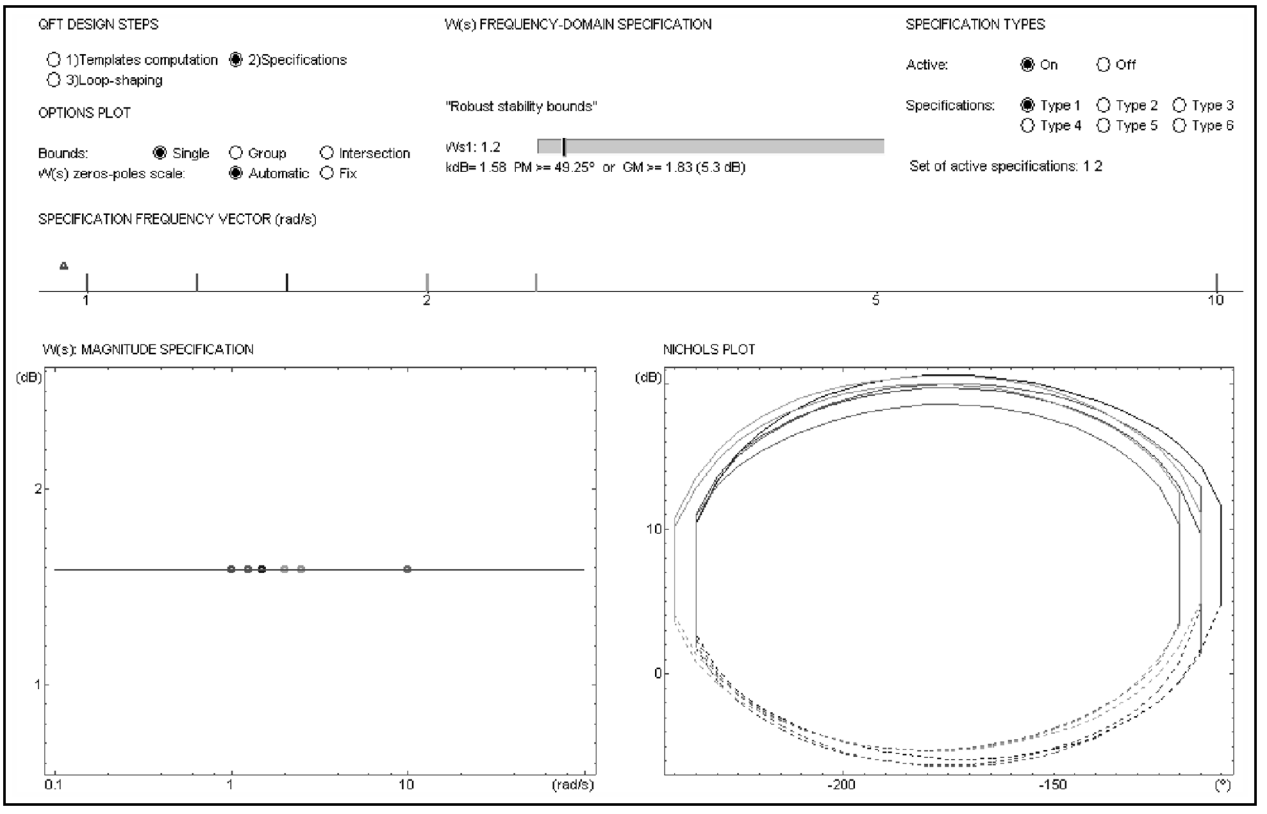

Figure 5. Aspect of the QFTIT window after configuring the robust stability specification for Problem 1.

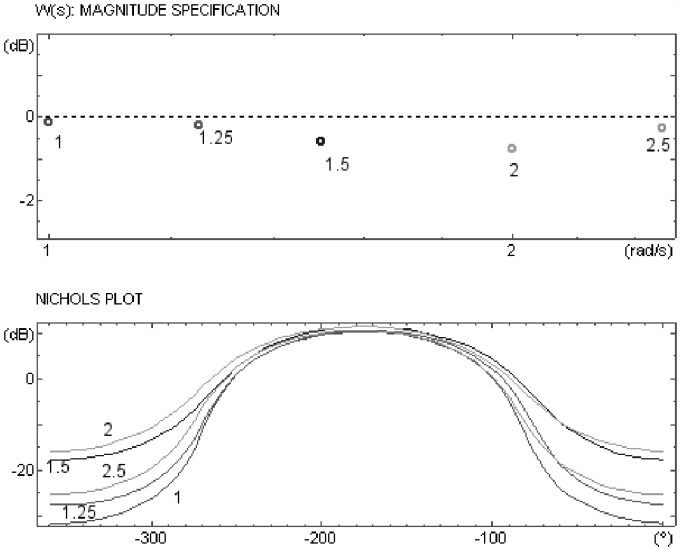

Figure 6. Aspect of the QFTIT window after configuring the specification of disturbance rejection at plant output (see table 1) for Problem 1.

It is a controller with two real zeroes, one real pole and a pair of complex poles. The zeroes and the poles of $C(s)$ are represented in the $C(s)$: zeros-poles zone (see figure 7).

4.5. *Stage 4: Validation*

During this stage designers make sure that the specifications of their design are fulfilled. The user only has to

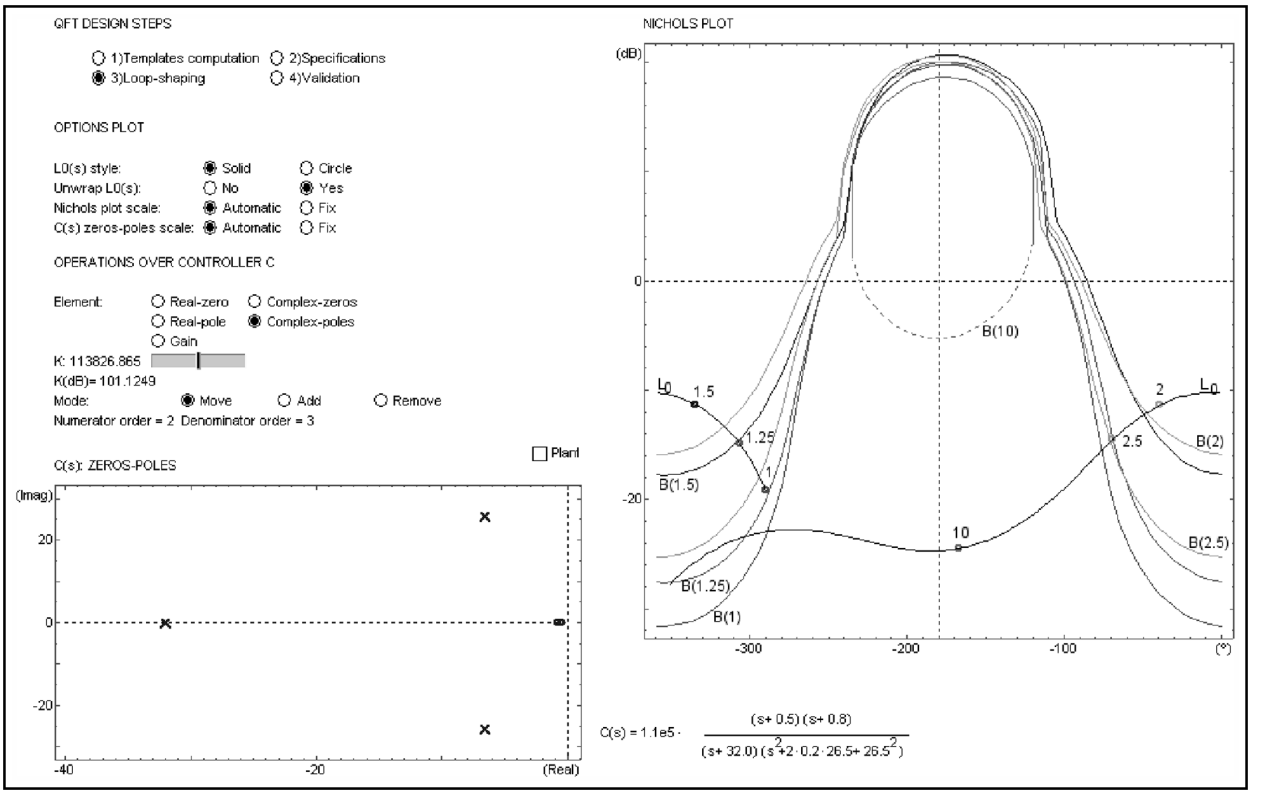

Figure 7. Aspect of the QFTIT window after designing the controller C for Problem 1.

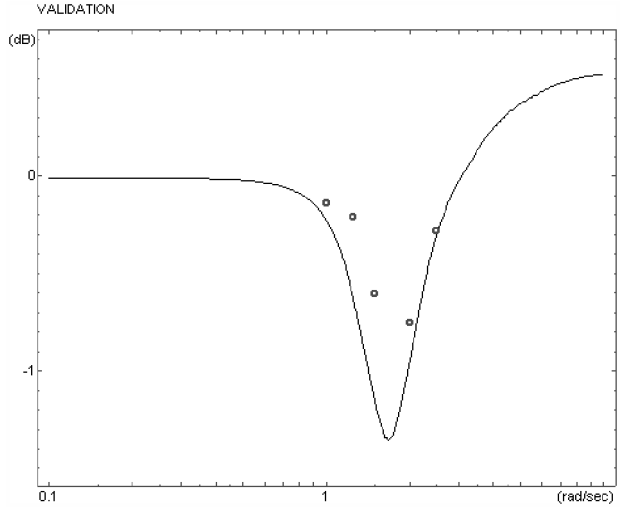

Figure 8. Maximum magnitude in dB of the maximum magnitude of the sensitivity function $\max\{|S(j\omega)|\}$ (solid line) and $W_d(\omega)$ (circles).

select the type of specification to validate, and QFTIT immediately shows the modulus of W_{si} and the worst case modulus of the associated characteristic function of the system (see table 2) in a Bode magnitude diagram.

For Problem 1, two specifications have to be validated: disturbance rejection at plant output (14) and robust stability (16). Figure 8 displays $W_d(\omega)$ (circles) and the maximum magnitude of the sensitivity function $\max\{|S(j\omega)|\}$ (solid line). It can be observed how the specification of disturbance rejection at plant output (14) is fulfilled, since $\max\{|S(j\omega)|\}$ is below $W_d(\omega)$ in the design range of frequencies $\Omega = [1,2.5]$ (rad/s).

On the other hand, figure 9 shows the maximum magnitude in dB of the closed-loop transfer function $\max\{|L(j\omega)/(1+L(j\omega))|\}$ and the constant gain line $W_s = 1.2$ (1.58 dB). As $\max\{|L(j\omega)/(1+L(j\omega))|\}$ does not surpass the horizontal line in any of the frequencies, the robust stability specification would be correct with the controller C designed during step 3. This design assures a phase margin $PM \geq 50^\circ$ and a gain margin $GM \geq 1.8$.

Time simulation of the non-linear process was done at four working points (ship speed $U = 30, 40$ knots and sea state number $SSN = 4, 5$). Table 3 shows the reduction percentages obtained in the average vertical acceleration WVA and motion sickness incidence MSI. The designed controller ensures a lower limit around 11.4% of reduction in MSI.

Moreover, it is interesting to compare the WVA and MSI percentage reductions obtained in the simulation

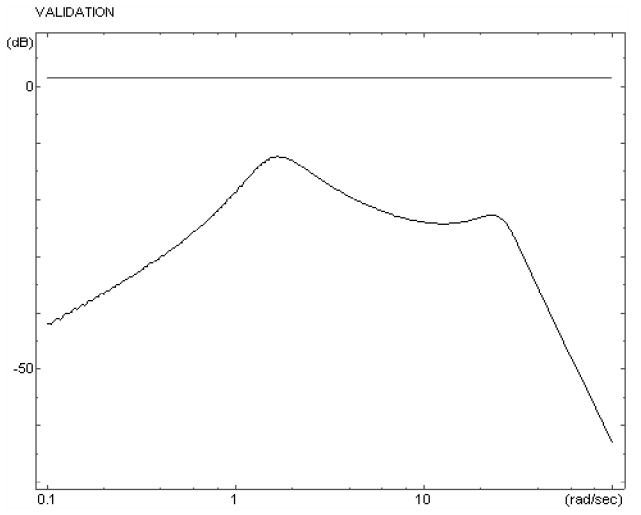

Figure 9. Maximum magnitude in dB of the closed-loop transfer function $\max\{|L(j\omega)/(1+L(j\omega))|\}$ and the constant gain line $W_s = 1.2$ (1.58 dB).

Table 3. WVA and MSI reduction percentages obtained in simulation.

(U, SSN)	WVA	MSI
(30, 4)	12.5%	25.4%
(30, 5)	10.9%	11.4%
(40, 4)	17.1%	31.8%
(40, 5)	15.3%	14.0%

Table 4. Reduction percentages of the MSI obtained in the simulation of the non-linear process using a gain-scheduling scheme with PD and the designed controller C with QFT.

(U, SSN)	MSI(PD)	MSI(C)
(30, 4)	40.3%	25.4%
(30, 5)	12.9%	11.4%
(40, 4)	40.7%	31.8%
(40, 5)	14.2%	14.0%

of the non-linear process using the gain-scheduling scheme with PD proposed in Díaz (2002) and the controller C obtained with QFT.

In table 4 it can be observed how better reduction percentages are obtained at the four working points with the gain-scheduling scheme with PD than with the controller C designed with QFT. This result was to be expected since QFT works with an infinite family of plants and produces a robust control design, thereby ensuring minimum features for all the family of plants. QFT is a more conservative design than the gain-scheduling scheme with PD, tuned optimally for only four working points.

Figure 10. Scaled down replica 1/25 the size of a high-speed ferry in El Pardo Model Basin (Spain).

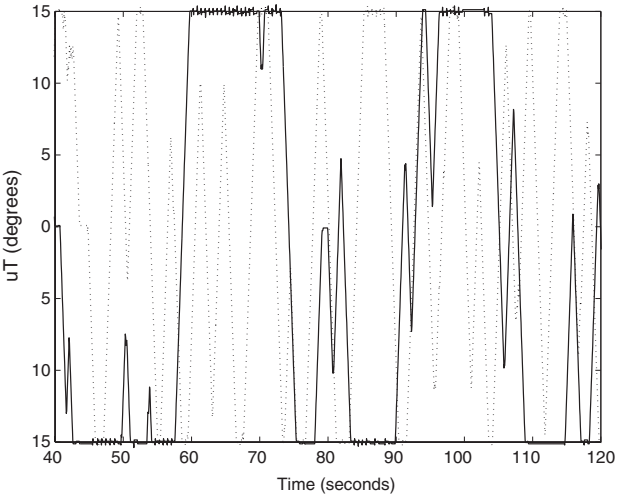

Figure 11. Position of the T-Foil measured in a sea behaviour trial at U = 40 knots and SSN = 4 using a PD controller (solid line) and using the robust controller C (broken line).

5. Experimental testing of the designed controller

In order to complete the validation of the design controller C, several sea behaviour trials in El Pardo Model Basin (Spain) were done at 40 knots and sea state number SSN = 4, 5 with a scaled down replica 1/25 the size of a high-speed ferry (see figure 10).

Figure 11 shows the position of the actuator (T-Foil) measured in a sea behaviour trial at 40 knots and SSN = 4 using a PD and the robust controller C. The saturation of both actuators is very high using the PD, while with the robust controller C there is almost no saturation. This behaviour is basically to be expected, since the controller C was designed to assure moderate saturation.

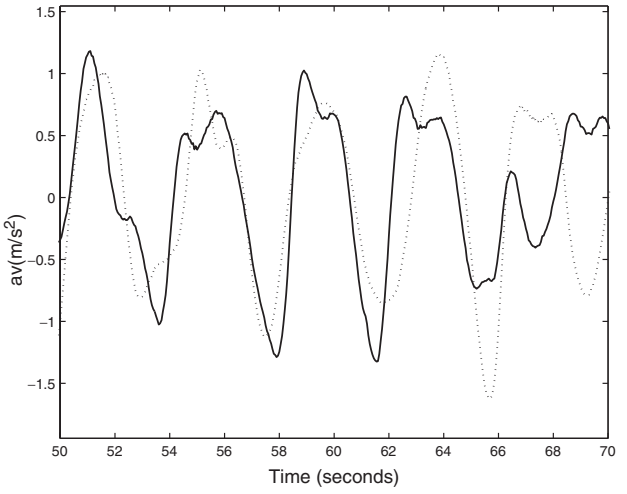

Figure 12. Vertical acceleration obtained in a sea behaviour trial at U = 40 knots and SSN = 4 of the process without control (broken line) and with the controller C (solid line).

Table 5. Reduction percentages of the MSI obtained in the sea behaviour trials using a gain-scheduling scheme with PD and the designed controller C.

(U, SSN)	MSI(PD)	MSI(C)
(40, 4)	20.4%	26.9%
(40, 5)	11.7%	10.3%

On the other hand, figure 12 shows the vertical acceleration obtained in sea behaviour trials at nominal conditions, with no control and using the robust controller C. A 12.2% reduction is achieved using this regulator.

Table 5 presents the MSI reduction percentages obtained with a gain-scheduling scheme using a PD controller, and with the robust controller C. It can be seen that at SSN = 4 the greatest MSI reduction is obtained with the robust controller C, while at SSN = 5 the MSI reduction obtained with both controllers is very similar. These results confirm the robust nature of the controller C and the strong dependency of the PD controller on the process model used for tuning it. To obtain a greater MSI reduction with the PD controller, it would have to be tuned again on the real process.

If tables 4 and 5 are compared, it can be observed that the MSI reduction percentages obtained in simulation are greater than the MSI reduction percentages obtained in sea behaviour trials for both controllers. This result is not strange because the process model used in simulation is only an approximation of the real process. However, the difference between MSI reduction obtained in simulation and MSI reduction obtained in the sea behaviour trials is smaller for the controller C due to its robust nature.

6. Conclusions

This work presents the monovariable design of a robust controller C using QFT to reduce motion sickness on a high-speed ferry. Motion sickness is caused by vertical accelerations associated with the heave and pitch motions induced by the waves. In a first approximation, the vertical acceleration associated with pitch motion can be considered as the sole cause of motion sickness. Therefore, the multivariable robust regulation problem can be reduced to a monovariable one.

The different stages of QFT methodology have been done with the help of QFTIT. It shows the utility of this free software tool for solving real design problems. QFTIT is characterized by its ease of use and interactive nature. Any actions carried out on the screen are immediately reflected on all the graphs generated and displayed by the tool. This allows designers to visually perceive the effects of their actions during the design of the controller. Moreover, control engineers quickly learn which parameter to use and how to push the design in the direction of fulfilling better tradeoffs in the specifications.

Testing of the controller C in sea behaviour trials using a scaled down replica 1/25 the size of a high-speed ferry in El Pardo Model Basin (Spain) showed the validity of the design, since acceptable MSI reduction percentages were obtained.

The designed controller C was compared with a previous one – a gain-scheduling scheme with PD. The comparison showed that the system controlled with C had robust performance, and presented low saturation of the actuators. On the other hand, the system controlled with a gain-scheduling scheme with PD presented a higher saturation and did not have any robust performance. This result was to be expected since QFT methodology works with a large family of plants and produces a robust control design, thereby ensuring minimum features for all the family of plants. It is a more conservative design than the gain-scheduling scheme, which uses classic controllers tuned exclusively at four working points.

The QFT monovariable robust design presented in this work is useful for the following reasons:

(1) It reduces MSI in an acceptable way using a sole actuator, the T-foil. Thus, it is possible to use the flaps to correct the course deviations, or even not to install them. Such kind of design was demanded for the naval industry, which prefers to install few mechanical actuators in the hull.
(2) It is the first design of this kind to solve the problem of the MSI decreasing. Therefore, it can be a reference for futures designs of the same kind.

(3) It is an advisable previous step for the successful realization of a QFT multivariable robust design. It gives valuable information an experience about how to translate the specifications to the frequency domain, and how to try to do the loop-shaping in the Nichols diagram.

Acknowledgments

This work was supported by the Spanish CICYT under grants DPI2003-09745-C04-01 and DPI2004-01804.

References

J. Aranda, J.M. Cruz and J.M. Diaz, ''Identification of multivariable models of fast ferries'', *European Journal of Control*, 10(2), pp. 187–198, 2004.

J. Aranda, J.M. Cruz and J.M. Diaz, ''Design of a multivariable robust controller to decrease the motion sickness incidence in fast ferries'', *Control Engineering Practice*, 13(8), pp. 985–999, 2005.

K.J. Åström, ''The future of control'', *Modeling, Identification and Control*, 15(3), pp. 127–134, 1994.

K.J. Åström, ''Limitations on control system performance'', *European Journal of Control*, 6(1), pp. 2–20, 2000.

C. Borghesani, Y. Chait and O. Yaniv, *Quantitative Feedback Theory Toolbox – for use with MATLAB*, Natick, MA: The MathWorks Inc., 1995.

Y. Chait and O. Yaniv, ''Multi-Input/single-output computer aided control design using the Quantitative Feedback Theory'', *International Journal of Robust and Nonlinear Control*, 3, pp. 47–54, 1993.

J.M. Cruz, J. Aranda, J.M. Giron-Sierra, F. Velasco, S. Esteban, J.M. Diaz and B. Andres-Toro, ''Improving the comfort of a fast ferry, smoothing a ship's vertical motion with the control of flaps and T-foil'', *Control Systems Magazine*, 24(2), pp. 47–60, 2004.

J.M. Diaz, ''Identification, Modelling and control of the vertical dynamics of a high speed ship'', Doctoral thesis, Distance University of Spain (UNED), Madrid, Spain, 2002.

S. Dormido, ''The role of interactivity in control learning (Plenary Lecture)'', in *Proceedings of the IFAC Symposium on Advances Control Education ACE'03*, Oulu, Findland, June, 2003.

S. Dormido, ''Control learning: Present and future'', *Annual Reviews in Control*, 28, pp. 115–136, 2004.

S. Esteban, J.M. Giron-Sierra, J.M. Cruz, B. Andres, J.M. Diaz and J. Aranda, ''Fast ferry vertical accelerations reduction with active flaps and T-foil'', in *Proceedings of 5th IFAC Conference on Manoeuvring and Control of Marine Craft* (*MCMC2000*), Aalborg, Norway, 23–25 August 2000, pp. 233–238.

P.O. Gutman, C. Baril and L. Neumann, ''An algorithm for computing value sets of uncertain transfer functions in factored real form'', *IEEE Transactions on Automatic Control*, 29(6), pp. 1268–1273, 1995.

I.M. Horowitz, *Synthesis of feedback systems*, New York: Academic Press, 1963.

I.M. Horowitz, *Quantitative feedback design theory* (*QFT*), QFT Publishers, 660 South Monaco Dorkway Denver, Colorado. 80224–1229, 1992.

I.M. Horowitz, ''Survey of Quantitative Feedback Theory (QFT)'', *International Journal of Robust and Non-linear Control*, 11(10), pp. 887–921, 2001.

C.H. Houpis, R.R. Sating, S. Rasmussen and S. Sheldon, ''Quantitative feedback theory technique and applications'', *International Journal of Control*, 59, pp. 39–70, 1992.

C.H. Houpis and S. Rasmussen, *Quantitative Feedback Theory: fundamentals and applications*, New York: Marcel Dekker, 1999.

J.F. O'Hanlon and M.E. McCauley, ''Motion sickness incidence as a function of the frequency and acceleration of vertical sinusoidal motion'', *Aerospace Medicine*, 45(4), pp. 366–369, 1974.

Y. Piguet, *SysQuake: User Manual*, 2004, http://www.calerga.com

O. Yaniv, *Quantitative feedback design of linear and nonlinear control systems*, Norwell, Massachusetts: Kluwer Academic Publishers, 1999.